Analysis of lead-free piezoceramic based power ultrasonic transducers for wire bonding

Andrew Mathieson*,Dominick A. DeAngelis†
*School of Engineering, University of Glasgow, Glasgow, G12 8QQ, UK
†Mechanical Engineering, Ultrasonics Group, Kulicke & Soffa Industries Inc., Fort Washington, PA 19034, USA

***Abstract*—Since the 1950s, lead zirconium-titanate (PZT) has been the dominant transduction material utilized in power ultrasonics, while lead-free piezoceramics have been largely neglected due to their relatively poor piezoelectric and electromechanical properties. However, the implementation of environmental directives that regulate and control the use of hazardous materials, such as lead, triggered a search for new high performance lead-free piezoceramics. Recent advances have led to lead-free piezoceramics exhibiting properties similar to PZT, but despite this, reports utilizing these novel piezoceramics in practice are limited. This research employs a modified variant of bismuth sodium titanate (BNT) in a power ultrasonic transducer used for metal welding during the manufacture of semiconductors. The important factors for transducer reliability and performance are investigated, such as piezoceramic aging and stack preload level. It is reported that BNT based transducers exhibit good stability, and can withstand a stack preload level of 90 MPa without depoling. Although the BNT based transducers exhibited larger dissipative losses compared to identical PZT8 based transducers, the tool displacement gain was larger under constant current conditions. Semiconductor wire bonds which satisfied the commercial quality control requirements were also formed by this BNT based transducer.**

***Index Terms*—Lead-free piezoceramic, BNT, power ultrasonic transducer, wire bonding**

I. Introduction

Lead-free ferroelectric ceramics were first reported in the early 1940s, with the first ultrasonic transducers based on barium titanate (BT) developed in 1947. BT was the first piezoceramic that could be practically utilized in ultrasonic transducers. However, it was largely superseded during the early 1950s by lead zirconate-titanate (PZT), when it was shown to exhibit superior piezoelectric and electromechanical properties to BT [1-3]. PZT and its variants are currently the dominant piezoceramic material adopted in ultrasonic applications. Even other lead-free piezoceramics which possess improved properties to BT, such as alkaline niobates (KNN) and bismuth-sodium titanates (BNT) which were developed during the 1950s the early 1960s respectively [4, 5], could not compete with PZT. As a consequence, these lead-free piezoceramics have been largely neglected by the research community in the second half of the 20th century [6].

An upsurge in academic interest in lead-free piezoceramics during the last decade indicates that significant scientific and financial resources have been employed in the development of these materials [6-8]. This increased interest can be largely accredited to the adoption of two European Union (EU) directives; 2002/96/EC "Waste electrical and electronic equipment (WEEE)" [9] and 2002/95/EC "The Restriction of the use of certain Hazardous Substances in Electrical and Electronic Equipment (EEE) directive" (RoHS) [10]. While WEEE was implemented to tackle Europes increasing quantity of electrical and electronic waste, RoHS bans the introduction of new EEE products entering the EU marketplace if they contain more than a certain percentage of four heavy metals, one of which is lead (0.1%), and two flame retardants. The popularity of lead-based piezoceramics and their increased adoption in engineering applications risks the release of more and more lead into the environment through lead oxide (which is expelled during manufacture) or during disposal at end of life [6, 7]. Lead-based piezoceramics such as PZT typically contain 60 %wt lead, and hence do not conform to RoHS. Exemptions to these directives can be granted if an equivalent substitute material is not available, if the substitute is impractical or would negatively affect the socioeconomic, health or safety of the consumer. PZT has been granted such an exemption from the original and amended RoHS directives [10, 11] due to the lack of an available lead-free substitute. However, this exemption is currently under review, with a decision for its extension due by July 2016. Although it is likely that lead-based piezoceramics will continue to enjoy exemption from this directive post 2016, it is possible this exemption could be rescinded during future reviews.

Two of the most promising families of lead-free piezoceramics for power ultrasonic applications are alkaline niobates (KNN) and bismuth-sodium titanates (BNT) [5, 7-8]. A significant breakthrough was made in 2004 when it was reported that a modified KNN piezoceramic exhibited a piezoelectric charge constant, d_{33}, which was five times larger than previously observed in KNN piezoceramics [12]. While this piezoceramic displayed properties associated with 'soft' PZT piezoceramics, it was later reported that altering its manufacturing technique [13] and acceptor doping gave KNN piezoceramics the potential to exhibit piezoelectric properties and a mechanical quality factor, Q_m, which are comparable with hard piezoceramics [14]. Additionally, it has also been reported that BNT piezoceramics have also exhibited Q_m, coupling coefficients k_t and k_p, and dissipation factor, tan δ, which are comparable to hard PZT after acceptor doping with manganese [15, 16]. However, lead-free piezoceramics

This project was funded by the Glasgow Research Partnership in Engineering (GRPE). Manuscript received 13th August 2015; revised 28th October 2015. Corresponding author: A. Mathieson (email: andrew.mathieson@glasgow.ac.uk).

developed for power applications have also demonstrated low sensitivity and typically exhibit a d_{33} that is significantly lower than normally observed in hard PZT piezoceramics [14, 16].

Although studies discussing the incorporation of lead-free piezoceramics in power ultrasonic devices are limited, variations of alkaline niobates and bismuth-sodium titanates have been reported to have been successfully employed in Langevin-type transducers for use in wire bonding [17, 18]. These studies illustrated that lead-free piezoceramics could be successfully incorporated into a device, and that a lead-free transducer could produce wire bonds. This investigation also demonstrates that wire bonds can be successfully formed by a commercial power ultrasonic transducer based on a lead-free piezoceramic, specifically a variant of BNT. It also extends this research to transducer design, such as transducer preloading, which has not before received significant attention for lead-free based devices. Transducer preloading significantly influences the performance and reliability of devices. Excessive preloading can induce piezoceramic depoling and failure in the tensile bolt (in conventional Langevin-type transducers), while insufficient preloading can cause fatigue failure within piezoceramic elements and increase losses within the piezoceramic stack. It is therefore crucial that preloading is well understood before reliable lead-free devices are manufactured on a commercial scale.

II. Piezoceramic material

Five samples of BNT (PIC700, PI Ceramic GmbH) and PZT8 plates with approximate dimensions of 6.5 x 4.5 x 1 mm, were analyzed, and their properties are presented in Table 1. The impedance, Z_{fs}, of each sample was measured with a spectrum analyzer (HP E5100A) at the series resonant frequency, f_s, of their length, width and thickness modes of vibration, while k_{eff} was calculated from the collected impedance data. Due to the aspect ratio of the piezoceramic plate, the thickness mode couples with higher order transverse modes of vibration. The capacitance and tan δ where measured at 1 kHz using an LCR meter (BK Precision 878).

From Table 1, it can be seen that the resonant frequencies of the BNT piezoceramic plates are higher than those of the PZT8 plates. This can be attributed to BNT possessing a lower density, as presented in Table 1, and higher acoustic velocity (~ 4290 ms^{-1}) than PZT8 ($\sim$3120 ms^{-1}). It can also be observed that Z_{fs} and tan δ are significantly higher in the BNT plates than the PZT8 plates. Combined with a notably lower Q_m and k_{eff}, it is expected that BNT piezoceramic will display higher losses and will not be as efficient at converting electric energy to strain compared to PZT8. The k_{eff} of the thickness mode could not be calculated due to the high spectral density of transverse modes of vibration in close proximity to the thickness mode. However, the lower capacitance value measured in the BNT samples indicates that it will exhibit lower sensitivity than PZT8 samples. This is confirmed by the investigated BNT variant exhibiting a lower value of d_{33} when compared to PZT8, as shown in Table 1.

The magnitude variation across the measured properties of both the BNT and PZT8 plates are also presented in Table 1. The variation of the parameters f_s, Z_{fs}, capacitance and tan δ across the BNT plates are mostly comparable with those measured from the PZT8 plates. This suggests that batches of transducers employing the investigated BNT piezoceramic could be fabricated without large variations in their resonant frequency and impedance properties: a crucial consideration in commercial transducer manufacture.

III. Unibody transducer

The BNT transducer and PZT8 transducer are shown in Fig. 1 in both unassembled and assembled form. The unibody design consists of a monolithic titanium body with a rectangular aperture designed to fit four piezoceramic plates and a titanium preloading wedge [21]. The main advantage of this transducer configuration is the high-uniformity of stress through the piezoceramic stack. The ratio between the maximum and minimum stress across the piezoceramic stack is less than 1.5 and is significantly less than typically observed in Langevin-type transducers. This permits the piezoceramic stack to undergo preloading which is approximately three times higher without depoling of the piezoceramic elements than typically applied in Langevin-type transducers that are preloaded via a central tensile bolt. This minimizes acoustic losses associate with the interfaces between the piezoceramic elements, shim electrodes and transducer body. The piezoceramic elements in the PZT8 based transducer were preloaded to 95 MPa, the preload specification of commercially fabricated devices. As the properties of BNT variants are strongly influenced by the application of stress [22], a suitable preload for a transducer based on this variant of BNT was unknown. Therefore, a range of preloads were investigated comprising of 30 MPa, 50 MPa, 60 MPa and 90 MPa. All experimental measurements were conducted with the transducers mounted by their support flange, in a similar configuration as their in situ operational constraints. A ceramic capillary tool, the part through which the bond wire passes and forms the bond, was also fastened to each transducer.

A. Resonant frequency identification

Modal parameters of the transducers, comprising resonant frequency and modes of vibration, were identified through experimental modal analysis (EMA). The vibrational response of each device was measured across a grid of points in the out-of-plane direction using a scanning 1D laser Doppler vibrometer, LDV, (Polytec PSV-200). A pseudo random signal, generated by the function generator integrated into the vibrometer control, was used to excite the transducers before Polytec VibSoft Data Acquisition software and PSV Scanning Vibrometer Software Version 8.8 recorded, averaged, and extracted the modal data with a resolution of 15.6 Hz between 40 kHz and 200 kHz. To enable measurements to be simultaneously recorded across the front, side and top faces of the transducer body and capillary, mirrors were located to the top, left-hand side (LHS) and right-hand side (RHS) of the device. Fig. 2 illustrates the location of the mirrors with reference to the device, while superimposed contour plots, where blue indicates displacement towards the LDV and red

TABLE I
PARAMETERS MEASURED FROM THE BNT AND PZT8 PLATES† : SUPPLIED BY PI GMBH, ‡: AVERAGED CATALOG VALUES [20].

	f_s (kHz) Average	Upper/ lower limits	Z_{fs} (Ω) Average	Upper/ lower limits	k_{eff} Average	Upper/ lower limits	Capacitance (pF) Average	Upper/ lower limits	tan δ Average	Upper/ lower limits	Density (kg/m^3)	d_{33} (pC/N)	$\varepsilon^T{}_{33}/\varepsilon_0$	Q_m
BNT														
Length mode	346.4	+0.400 (+0.1%) -0.300 (-0.1%)	2176	+18 (+0.8%) -14 (-0.7%)	0.0578	+0.0082 (+14.2%) -0.0255 (-44.0%)								
Width mode	529.1	+0.563 (+0.1%) -0.322 (-0.1%)	998	+5 (+0.5%) -9 (-0.9%)	0.1148	+0.0028 (+2.4%) -0.0015 (-1.3%)	195	+0.6 (+0.3%) -0.4 (-0.2%)	0.024	+0.0016 (+6.2%) 0.0004 (-1.7%)	5600†	120†	700†	∼100†
Thickness mode	2455.1	+10.844 (+0.4%) -7.281 (-0.3%)	60	+2 (+3.2%) -2 (-3.5%)	-	- -								
PZT8														
Length mode	269.1	+0.194 (+0.1%) -0.194 (-0.1%)	28	+7 (+20.0%) -3 (-12.0%)	0.2111	+0.0011 (+0.5%) -0.0005 (-0.2%)								
Width mode	411.4	+0.201 (+0.1%) -0.149 (0.0%)	9	+1 (+10.0%) -0 (0.0%)	0.4330	+0.0022 (+0.5%) -0.0013 (-0.3%)	294	+6.2 (+2.1%) -4.8 (-1.7%)	0.002	0.0000 (0.0%) 0.0000 (0.0%)	∼7600‡	∼260‡	∼1000‡	∼1200‡
Thickness mode	2197.0	+5.972 (+0.3%) -4.809 (-0.2%)	9	+1 (+10.0%) -2 (-28.6%)	-	- -								

designates displacement away from the LDV, in the out-of-plane directions. It has been shown that the front of the transducer and the free-end of the capillary of the transducer exhibit the largest displacements at the operational mode of vibration, while small displacements observed in the side and top of the transducers can be accredited to Poissons effect. Fig. 2 also shows that the operational mode of vibration of the BNT and PZT8 transducer are identical. In addition to the operational mode of vibration, yaw modes of vibration (where the transducer body flexes from side to side) and a pitch mode of vibration (where the transducer body flexes up and down) were also identified.

B. Influence of transducer preload

The transducer parameters and the admittance and phase plots of the investigated devices one hour post preloading are presented in Table 2 and Fig. 3 respectively. These were measured and calculated using the same techniques as discussed in Section 2. A trend can be identified from Table 2 which indicates that as greater preload levels are applied to the BNT transducers, the higher its resonant frequency. This was expected, as the stiffness of the piezoceramic stack increased and hence losses associated with wave propagation reduced within the stack with preload level. However, it was also observed that the resonant frequency of the operational mode of vibration of each BNT based transducer does not significantly differ from the resonant frequency of the operational mode measured from the commercial PZT8 based transducer. Furthermore, when detected, the resonant frequencies of the yaw and pitch modes of vibration were also found at similar frequencies to those identified in the PZT8 transducer, Fig. 3. Considering the large differences between the resonant frequencies of individual piezoceramic plates presented in Table 1, this was not expected. This demonstrates that the resonant frequency of the transducer is dominated by the transducer body and stiffness of the piezoceramic stack, rather than the piezoceramic material incorporated within the device.

From Table 2 it is evident that preload level (within a range of 30 to 90 MPa) has a limited influence on the value of k_{eff} measured in the BNT transducers. This is contrary to results of a study that reported on a similar preload level in PZT8 based transducers with an identical unibody configuration as presented in Fig. 1 [23]. Below a preload of 60 MPa, it was found that the k_{eff} measured from the PZT8 transducers did not vary with preload level. However, above 60 MPa, the k_{eff} was measured to decrease with increasing preload. It is known that k_{eff} is sensitive to domain wall motion induced by the application of stress, suggesting that the PZT8 plates employed in the transducer in this investigation are demonstrating characteristics associated with depoling. In addition, Z_{fs} of the BNT transducers was found to reduce with increased preload. Although this was also observed in PZT8 transducers under similar conditions [23] up to a preload level of 60 MPa, Z_{fs} was measured to increase when the transducer was preloaded above 60 MPa. This suggests an increase of loss in PZT8, another indication that PZT8 piezoceramic plates are exhibiting depoling behavior. The stability of tan δ, which only varies by 8% across the investigated preload levels, is further evidence that the variant of BNT utilized in this study did not exhibit characteristics of depoling within the assessed

TABLE II
PARAMETERS MEASURED FROM THE INVESTIGATED TRANSDUCERS ONE HOUR AFTER PRELOADING.

	f_s (kHz)	Z_{fs} (Ω)	k_{eff}	Q_m	FOM	Capacitance (pF)	tan δ	Gain		
								μm per mA	μm per V	μm^2 per W
30 MPa BNT transducer	121.4	467	0.1049	227	2.5	783	0.033	0.0122	0.0217	0.2394
50 MPa BNT transducer	120.3	412	0.0999	317	3.2	799	0.035	0.0133	0.0301	0.3745
60 MPa BNT transducer	123.4	310	0.1118	355	4.4	807	0.034	0.0119	0.0342	0.3848
90 MPa BNT transducer	124.3	308	0.1049	389	4.2	826	0.036	0.0127	0.0368	0.4405
95 MPa PZT8 transducer	119.4	27	0.2707	375	27.5	1700	0.006	0.0038	0.1296	0.4912

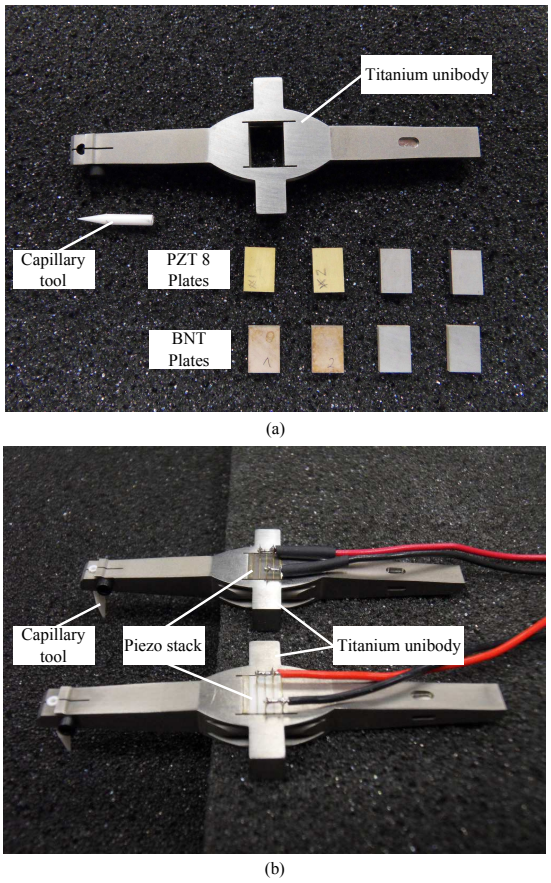

Fig. 1. (a) An unassembled unibody transducer, (b) Assembled transducers containing BNT (near) and PZT8 (far).

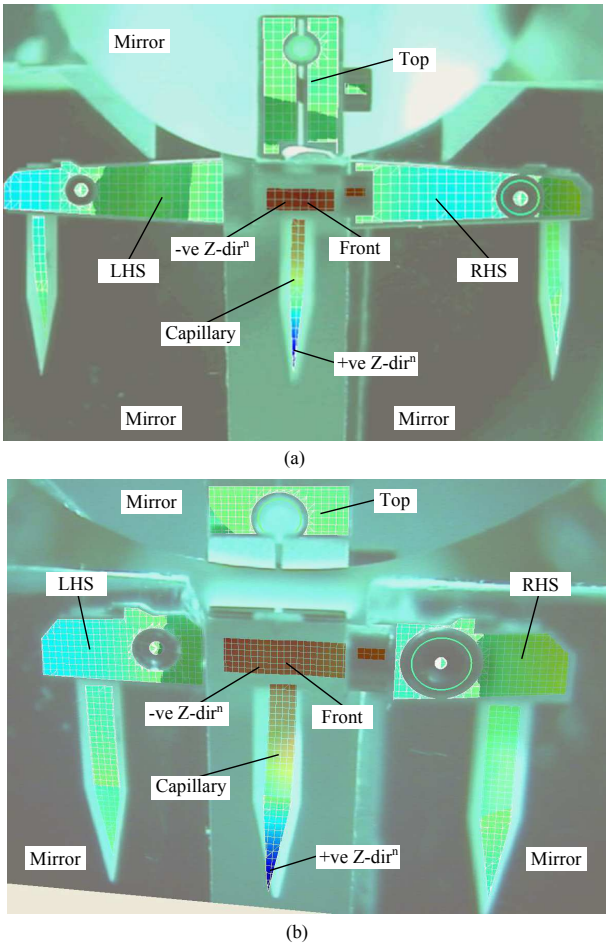

Fig. 2. Mode shape of the operational mode of vibration (positive Z direction vibrational motion towards LDV, negative Z direction vibrational motion away from LDV) for the (a) 50 MPa BNT transducer, and (b) PZT8 transducer.

preloading regime.

From Table 2, it is has also been shown that Q_m of the BNT transducers increases with preload level. This was also observed in PZT8 transducers [23], again indicating that this parameter is influenced by the transducer body and stiffness of the stack. Stack stiffness is primarily dominated by joint interfaces and as the contact area between two faces increases with preload, so does the stiffness of the stack [24]. Although Q_m measured from the 90 MPa BNT transducer and 95 MPa PZT8 transducer are similar, this does not suggest that both devices will have similar performance.

Parameters which indicate loss within a piezoelectric device, Z_{fs} and tan δ, were found to be considerably larger in the BNT transducers than those exhibited by the 95 MPa PZT8 transducer, while the lower capacitance of the BNT transducer was expected due to a significantly lower d_{33} measured from the BNT plates. However, it is the coupling coefficient that is the most important parameter when considering the performance of a power ultrasonic transducer, as it defines the capability of a piezoelectric material to convert mechanical stored energy into output energy [24]. A figure of merit (FOM), $k^2_{eff}.Q_m$, can be used to estimate the potential output velocity of a power ultrasonic transducer [8] and is presented for each transducer in Table 2. It can be seen that the k_{eff} of the 90 MPa BNT transducer is approximately 60% lower than the value measured from the 95 MPa PZT8 transducer. This significantly affects the FOM of the BNT transducers and suggests that the PZT8 transducer is likely to exhibit greater vibrational amplitudes for a given drive signal. This is also emphasized

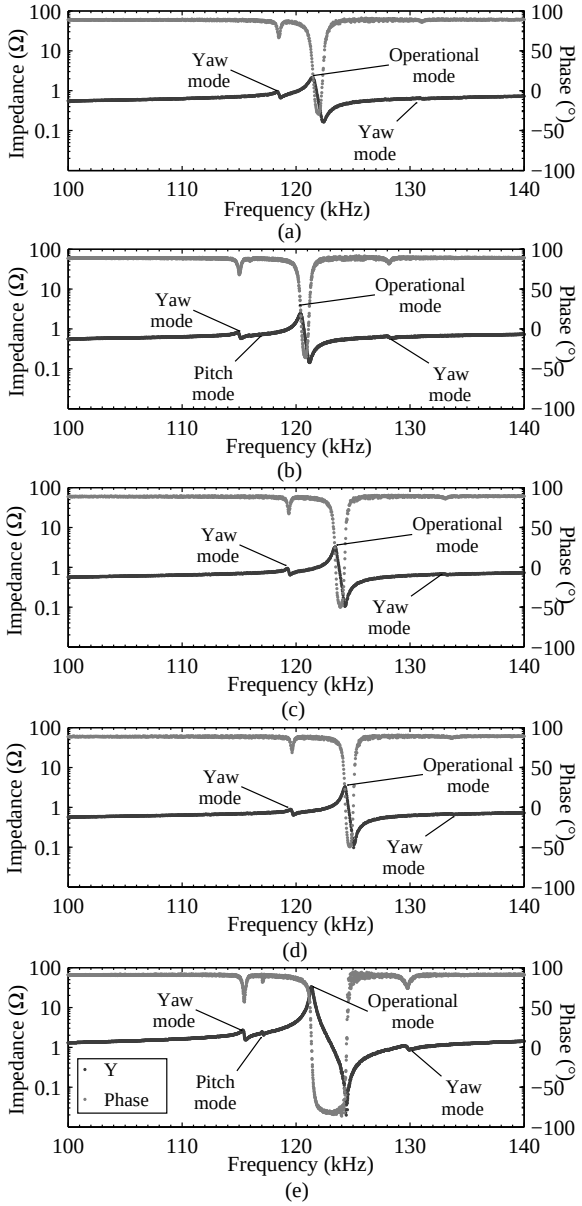

Fig. 3. Admittance and phase traces one hour after preloading for the (a) 30 MPa BNT transducer, (b) 50 MPa BNT transducer, (c) 60 MPa BNT transducer, (d) 90 MPa BNT transducer, and (e) 95 MPa PZT8 transducer.

by the respective admittance loops of the PZT8 and 90 MPa BNT transducers shown in Fig. 4. The size of the loop is also largely determined by k_{eff} and Q_m and it is clear from Fig. 4 that the PZT8 transducer exhibits a significantly larger loop than the 90MPa BNT transducer.

Preload level has a varying influence on the gain of the BNT transducers. Under a constant current condition (μm per mA), preload appears to have limited influence on the gain of the transducer, while under constant voltage (μm per V) and power conditions (μm^2 per W), the greater the preload, the higher the gain. This is likely attributable to the corresponding lowering of impedance of the transducers with increasing preload. The 95 MPa PZT8 transducer exhibits a gain 3.5 times larger than the 90 MPa BNT transducer under constant

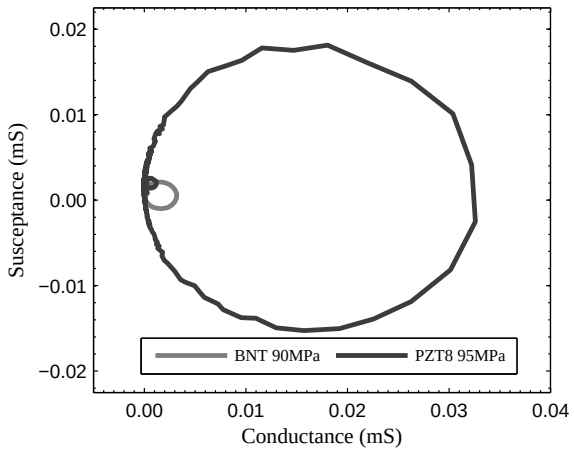

Fig. 4. Admittance loops of the 90MPa BNT transducer and 95MPa PZT8 transducer one hour after preloading.

voltage conditions, while under constant power conditions the BNT transducers and the PZT8 transducer exhibit similar gain values. However, under constant current conditions, the gain of the 90 MPa BNT transducers exhibit a gain 3.3 times larger than the PZT8 transducer. This is significant with respect to the wire bonding process, as the ultrasonic devices are driven under this condition. A similar observation was reported in another study investigating wire bonding transducers based on a different lead-free based piezoceramic, alkaline niobate (NKN). The enhanced performance was accredited to superior acoustic impedance matching between the end-masses of the transducer and the piezoceramic material [18]. However, similar to the BNT transducers investigated in this study, the NKN based wire bonding devices also exhibited high Z_{fs} [18]. The superiority of lead-free devices to exhibit elevated levels of gain whilst under constant current conditions may be partly explained by Ohms law and the capability of the driving system to draw an elevated voltage and a small current due to a higher Z_{fs}.

It has also been documented that the lead-free piezoceramics, including variants of BNT, exhibit blocking forces (the maximum force a piezoelectric element can generate under an electric field) which are equal or greater to those found in variants of PZT [8, 22, 25, 26]. This is likely to stem from the high coercive fields exhibited by lead-free piezoceramics [5-6, 8, 15, 16, 25] and indicates that domain wall motion is more restricted in lead-free piezoceramics than lead-based piezoceramics. It is reasonable to conclude that the greater resistance to depoling exhibited by the BNT transducers stems directly from the inherently high coercive field exhibited by lead-free piezoceramics.

C. Transducer aging

The 50 MPa BNT transducer was analyzed over duration of one month to investigate whether an extended length of preloading, exposure to thermal loading and operational drive conditions induced aging in the transducer. Fig. 5 presents data collected from the transducer during this study. The markers

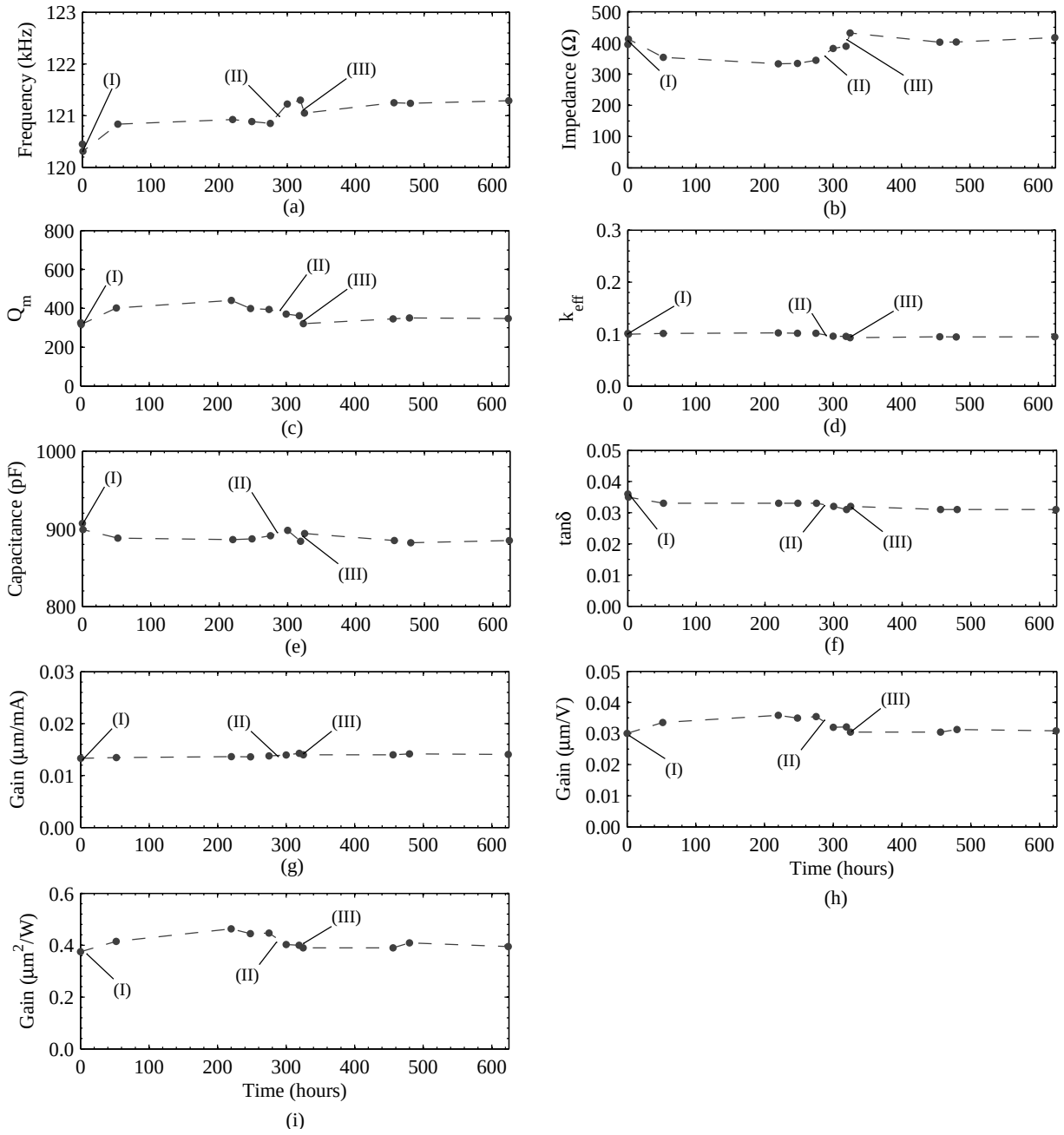

Fig. 5. Properties of the 50 MPa BNT transducer measured over a duration of 1 month (a) f_s, (b) Z_{fs}, (c) Q_m, (d) k_{eff}, (e) Capacitance, (f) tan δ, (g) Gain: constant current, (h), Gain: constant voltage, and (i) Gain: constant power.

indicate the parameters measured from driving the transducer under wire bonding conditions post pre-loading to assess the gain of the transducer (I), exposure to thermal loading at 70°C for 18 hours in an industrial oven (II), and both the BNT and the PZT8 transducers driven for an extended duration (20 seconds) under operational conditions (III).

From Fig. 5 it is clear that parameters such as k_{eff} and gain (measured under constant current) were stable throughout the measurement window, and varied little with respect to time, operational drive conditions or thermal loading. Other parameters such as Z_{fs}, Q_m, and gain, measured under constant voltage and constant power, varied with time and exposure to thermal loading (II). However, these parameters stabilized after 300 hours when the transducer was driven for an extended duration under operational conditions (III). The capacitance and tan δ values of the transducer also varied little with respect to time, despite both exhibiting sensitivity to thermal loading (II). After exposure to 70°C for 18 hours, 130°C below the maximum suggested operating temperature of the piezoceramic [19], tan δ and capacitance decreased and increased respectively. Driving the device under operational conditions (III) returned tan δ and capacitance (therefore d_{33}) to a similar value measured before (II).

The f_s of the BNT transducer varied during the initial 51

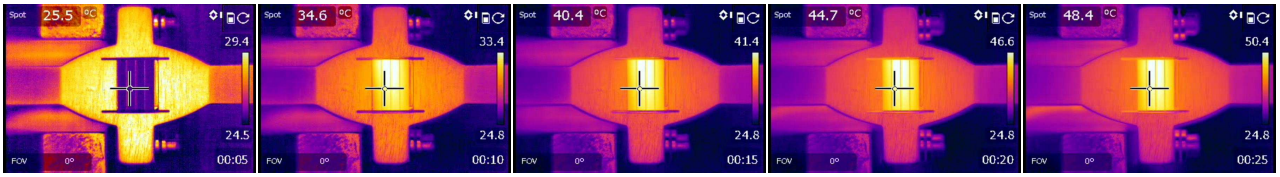

(a) (b) (c) (d) (e)

Fig. 6. Infra-red images of the BNT transducer driven at 2.2μm after (a) 0s: 25.5°C, (b) 5s: 34.6°C, (c) 10s: 40.4°C, (d) 15s: 44.7°C, (e) 20s: 48.4°C.

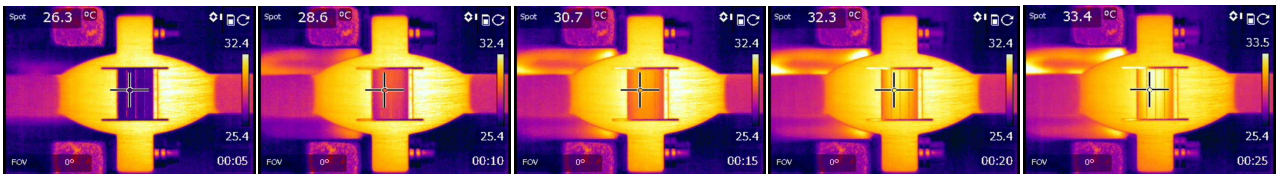

(a) (b) (c) (d) (e)

Fig. 7. Infra-red images of the PZT8 transducer driven at 2.2μm after (a) 0s: 26.3°C, (b) 5s: 28.6°C, (c) 10s: 30.7°C, (d) 15s: 32.2°C, (e) 20s: 33.4°C.

hours post preloading, increasing by 525 Hz, before stabilizing at approximately 120.9 kHz. However, thermal loading also influenced f_s causing an increase in resonant frequency. Driving the device under operational conditions (III) induced f_s to return to a lower frequency of 121.3 kHz, where its frequency stabilized.

The piezoceramic stack temperature from driving the devices under operational conditions were recorded using a Flir T440 infra-red camera and are illustrated in Fig. 6 and Fig. 7 and are depicted in the accompanying multimedia content. Considering the FOM of both transducers, it was expected that heating within the piezoceramic stack of the BNT transducer would be significantly greater. However, this is unlikely to be the fundamental factor limiting the adoption of BNT in commercial wire bonding power ultrasonic transducers. Temperature increases in the piezoceramic stack during wire bonding processes are likely to be not as large as those observed in Fig. 6 and Fig. 7. This is because only a short duty cycle (approximately 10% or 5 milliseconds) is required to form a bond and this excitation duration is unlikely to be significant. Piezoceramic stack heating is more likely to become problematic in power ultrasonic applications where devices to be driven for extended durations, such as ultrasonic cutting, and where power and vibrational amplitude requirements are greater.

The greatest limitation for the incorporation of BNT transducers into the wire bonding process is likely to stem from the small admittance loop of the transducer, as shown in Fig. 4. To ensure the transducer is driven under optimal conditions during the bonding process, a phase lock loop (PLL) tracking algorithm is utilized to track the frequency at which the transducer crosses zero phase. Due to the small admittance loop observed in the BNT transducer, the admittance curve did not always cross zero phase, with the effect that the algorithm could not identify the correct frequency to drive the transducer. This was corrected under bench test conditions by using capacitance compensation in the PLL drive circuit.

IV. Wire Bonding Analysis

To form wire bonds the 90 MPa BNT transducer was installed into an IConn^{TM} ProCu^{TM} (Kulicke and Soffa Industries Inc.) wire bonder. This machine produces ball type wire bonds from copper or gold wire in the manufacture of semiconductors. The copper or gold wire, typically in the order of 20 μm, is passed through the capillary tool of the ultrasonic transducer via a tension-controlled wire feed system for producing precise interconnecting wire loops. An electric spark, referred to as electric flame off (EFO), is applied to the end of the wire to form a ball shape via melting, before ultrasonic energy is applied, via micrometric vibrations generated at resonance by the transducer, to weld the ball to aluminum semiconductor die pad. This joining processes forms an intermetallic alloy between the pad substrate and wire. For the most common copper wire ball bonding applications, the capillary 'scrubs' the surface of the pad in an environment of inert gas to displace the aluminum oxide layer and expose the aluminum alloy substrate. The displaced oxide layer is referred to as 'splash', and for a feasible bond the splash should remain within the pad to minimize probability of a short circuit occurring between neighboring bonds.

The 90 MPa BNT transducer was used to form bonds with both gold wire and palladium coated copper wire. Fig. 8 presents a photograph of the copper wire bonds located on a semiconductor as well as scanning electron microscope (SEM) images of the same bonds. The SEM images illustrate that the bonds are uniform and correctly formed, and the splash remains within the pad from which it stemmed. This indicates that it is unlikely that a short circuit would occur between neighboring bonds.

The shear strength of the ball bonds formed using gold and palladium coated copper wire were assessed by measuring the force required to shear the wire from the aluminum pad using a Nordson Dage series 4000 multipurpose bond tester. From Table 3, it is shown that for both wire types, the higher the relative ultrasonic power level, the greater the absolute shear strength and the shear strength per unit area (the actual

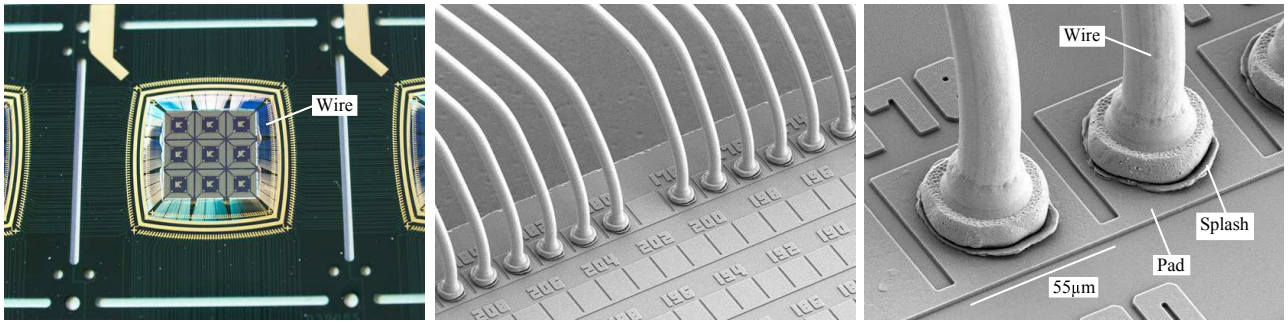

(a) (b) (c)

Fig. 8. Palladium coated copper wire ball bonds produced by the 90 MPa BNT transducer showing (a) Photograph of a semiconductor, (b) SEM image of wire bonds, and (c) Magnified SEM image of wire bonds.

TABLE III
AVERAGE RESPONSE OF 10 BONDS FORMED UNDER DIFFERENT RELATIVE ULTRASONIC POWERS.

Gold wire bonds			Copper wire bonds			
Relative ultrasonic power (%)	Absolute shear strength (g)	Shear strength per unit area (g/mm^2)	Relative ultrasonic power (%)	Absolute shear strength (g)	Shear strength per unit area (g/mm^2)	Intermetallic coverage (%)
50	9.3	5.1	80	16.2	7.0	51
60	11.3	5.9	85	17.6	7.6	63
70	12.9	6.4	90	18.0	8.0	66
80	13.8	6.4	95	18.8	8.1	72
			100	18.7	8.4	71

strength) of the bond; the ultrasonic power level is a unit that corresponds to the level of current supplied by the bonding machine to the transducer after device calibration, which ensures that bonds formed across a large number of bonding machines are identical. The results in Table 3 were also observed from bonds formed by commercial PZT8 transducers. The plateauing of the shear strength of the gold wire bond at 6.4 g/mm^2 corresponds with the maximum shear strength typically observed for gold wire bonds, and is independent of transducer type. Due to the low elastic and shear moduli of gold, a loading threshold is reached where the tool of the bond tester cuts through the wire ball, rather than shearing it from the pad. As copper has a significantly higher elastic and shear moduli than gold, greater bond strengths can be assessed, but unlike with gold the underlying pad structure is usually weaker than the bonded copper interface.

Intermetallic coverage (IMC) is an assessment of the intermetallic alloy formed by the chemical interaction between the wire and the aluminum pad, and is an indication of the actual bonded area. Fig. 9 depicts IMC after palladium coated copper wire bonds were formed at different relative ultrasonic powers. From Fig. 9, and from data presented in Table 3, it is evident that the percentage of IMC increases with respect to relative ultrasonic power. The percentage of IMC cannot be used to define bond strength due to variations in bond size, as larger bonds may have a low IMC percentage, but can still contain a larger surface area of IMC than small bonds with a high IMC percentage. However, when comparing the analyzed bonds, it can be stated in general that the larger the IMC, the stronger the bond.

The bonds analyzed in this study demonstrate characteristics that would be sufficient to satisfy quality control requirements for commercially formed bonds. Furthermore, it was observed that the 50 MPa transducer which was installed into the wire bonder machine exhibited a gain that was 1.7 larger than commercially manufactured PZT8 transducer. This indicates that if the wire bonder was fully optimized for the lead-free device, it is likely that the IMC and bond strength could be improved.

V. CONCLUSIONS

It has been demonstrated that a lead-free piezoceramic, a modified variant of BNT, whose parameters do not appear to suit power ultrasonic applications, can be successfully utilized in a commercial power ultrasonic device to perform industrial wire bonding. It has also been shown that under constant current conditions, which is the drive condition used during the wire bonding process, the BNT transducer exhibited a larger gain than a commercial transducer based on PZT. Furthermore, the BNT transducer displayed high level of stability, suggesting that the parameters of a BNT transducer could be predicted throughout the lifetime of the device. However, the BNT transducers exhibited high impedance and high dielectric losses which will negatively affect their practicality within industrial processes and these characteristics are likely to be the main factors that restrict their industrial adoption. It is also clear from literature and experimental findings presented in this study that further investigation is required to better understand what conditions, such as preload and temperature, enable optimal performance to be gained from power ultrasonic devices employing lead-free piezoceramics.

ACKNOWLEDGEMENT

Thanks to Eberhard Hennig of PI Ceramic GmbH, Germany, for support with the lead-free piezoceramic material and to

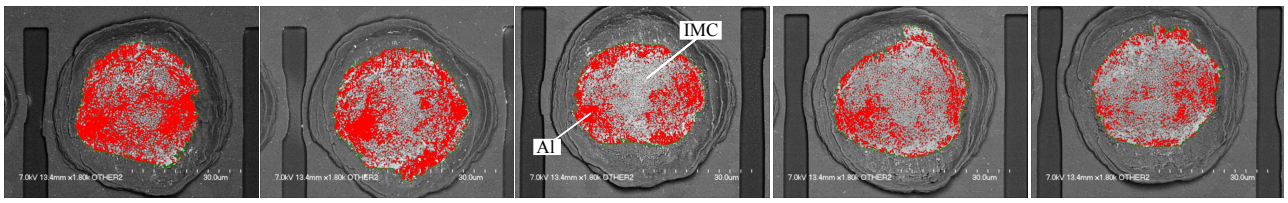

(a) (b) (c) (d) (e)

Fig. 9. IMC identified from SEM images of palladium coated copper wire bonds at relative ultrasonic powers (light shading indicates IMC, red indicates aluminum) of (a) 80%, (b) 85%, (c) 90%, (d) 95%, and (e) 100%.

Jon Brunner, K&S Fort Washington, PA, USA for configuring the wire bonding machine for the lead-free transducer and for assisting to analyze the feasibility of the wire bonds.

REFERENCES

[1] D.A. Berlincourt, "Piezoelectric transducer materials", *IRE Trans. on Ultrasonic Engineering*, vol. UE-4, pp. 53-65, 1956.

[2] H. Jaffe, D.A. Berlincourt, "Piezoelectric transducer materials", *Proceedings of the IEEE*, vol. 53, pp. 1372-1386, 1965.

[3] A.E. Crawford, "Lead zirconate-titanate piezoelectric ceramics", *Br. J. App. Phys.*, vol. 12, pp. 529-534, 1961.

[4] G. Shirane, R. Newnham, R. Pepinsky, "Dielectric properties and phase transitions of NaNbO3 and (Na, K)NbO3", *Phys. Rev.*, vol. 96, pp. 581-588, 1954.

[5] L. Pardo, "Piezoelectric ceramic materials for power ultrasonic transducers", in *Power Ultrasonics*, 1st ed. Cambridge, UK: Woodhead Publishing, 2015, ch. 5, pp. 101-125.

[6] J. Rödel, W. Jo, K.T.P. Seifert, E.-M. Anton, T. Granzow, D. Damjanovic, "Perspective on the development of Lead-free Piezoceramics", *J. Am. Ceram. Soc.*, vol. 92, pp. 11531177, 2009.

[7] J.F. Li, K. Wang, F.Y. Zhu, L.Q. Cheng, F.Z. Yao, "(K, Na) NbO3-based lead-free piezoceramics: Fundamental aspects, processing technologies, and remaining challenges", *J. Am. Ceram. Soc.*, vol. 96, pp. 3677-3696, 2013.

[8] J. Rödel, K.G. Webber, R. Dittmer, W. Jo, M. Kimura, D. Damjanovic, "Transferring lead-free piezoelectric ceramics into application", *J. Eur. Ceram. Soc.*, vol. 35, pp. 1659-1681, 2015.

[9] "Directive 2002/96/EC: Waste electrical and electronic equipment (WEEE)," *Off. J. Eur. Union*, pp. [L37] 24-38, 2003.

[10] "Directive 2002/95/EU: on the restriction of the use of certain hazardous substances in electrical and electronic equipment", *Off. J. Eur. Union*, pp. [L37] 19-22, 2003.

[11] Y. Saito, H. Takao, T. Tani, T. Nonoyama, K. Takatori, T. Homma, T. Nagaya, M. Nakamura, "Lead-free piezoceramics", *Nature*, vol. 432, pp. 84-87, 2004.

[12] E. Hollenstein, M. Davis, D. Damjanovic, N. Setter, "Piezoelectric properties of Li- and Ta-modified (K0.5Na0.5)NbO3 ceramics", *Applied Physics Letters*, vol. 87, pp.182905, 2005.

[13] S. Zhang, J.B. Lim, H.J. Lee, T.R. Shrout, "Characterization of Hard Piezoelectric Lead-Free Ceramics", IEEE Trans. Ultrason. Ferroelectr. Freq. Control, vol. 56, pp. 1523-1527, 2009.

[14] H.J. Lee, S.O. Ural, L. Chen, K. Uchino, S. Zhang, "High Power Characteristics of Lead-Free Piezoelectric Ceramics", *J. Am. Ceram. Soc.*, vol. 95, pp. 3383-3386, 2012.

[15] E. Taghaddos, M. Hejazi, A. Safari, "Electromechanical Properties of Acceptor-Doped Lead-Free Piezoelectric Ceramics", *J. Am. Ceram. Soc.*, vol. 97, pp. 17561762, 2014.

[16] H. Chan, S. Choy, C. Chong, H. Li, P. Liu, "Bismuth sodium titanate based lead-free ultrasonic transducer for microelectronics wirebonding applications", *Ceram. Int.*, vol. 34, pp.773777, 2008.

[17] T. Lee, K. Kwok, H. Li, H. Chan, "Lead-free alkaline niobate-based transducer for ultrasonic wirebonding applications", *Sensor. Actuat. A-Phys.*, vol. 150, pp.267-271, 2009.

[18] PI Ceramics data sheet [online]. Available: http://piceramic.com. Accessed February 2015.

[19] Morgan Ceramics data sheet [online]. Available: http://www.morganelectroceramics.com. Accessed February 2015.

[20] A. Safabakhsh (Assignee, Kulicke & Soffa Investments, Inc.), "Unibody Ultrasonics Transducer", US Patent 5 469 011, Nov. 21, 1995.

[21] R. Dittmer, K.G. Webber, E. Aulbach, W. Jo, X. Tan, J. Rödel, "Electric-field-induced polarization and strain in 0.94(Bi1/2Na1/2)TiO30.06BaTiO3 under uniaxial stress", *Acta Mater.*, vol. 61, pp. 1350-1358, 2013.

[22] D.A. DeAngelis, G.W. Schulze, "Optimizing piezoelectric crystal preload in ultrasonic transducers", *Ultrasonic Industry Association (UIA), 2009 38th Annual Symposium of the*, pp. 1-6, 23-25 March 2009.

[23] D. Stansfield, Underwater Electroacoustic Transducers, Peninsula Publishing, 1991.

[24] X. Tan, E. Aulbach, W. Jo, T. Granzow, J. Kling, M. Marsilius, H.-J. Kleebe, J. Rödel, "Effect of uniaxial stress on ferroelectric behavior of (Bi1/2Na1/2)TiO3-based lead-free piezoelectric ceramics", *J. Appl. Phys.*, vol. 106, pp. 044107, 2009.

[25] R. Dittmer, E. Aulbach, W. Jo, K.G. Webber, J. Rödel, "Large blocking force in Bi1/2Na1/2TiO3-based lead-free piezoceramics", *Scr. Mater.*, vol.67, pp. 100-103, 2002.

Andrew Mathieson was born in Glasgow, Scotland, in 1984. He obtained an M.Eng. degree in mechanical engineering in 2007 before completing a Ph.D. degree in 2012, both from the School of Engineering, University of Glasgow. His doctoral thesis investigated the vibrational behavior of power ultrasonic surgical devices with focus on their nonlinear responses. Presently, Andrew is working as a research associate in power ultrasonics group at the University of Glasgow, where his research interests include the application of power ultrasonics to medical and industrial applications. Andrew is a chartered engineer and Member of the Institution of Mechanical Engineers.

Dominick A. DeAngelis was born in Wilkes-Barre, Pennsylvania in 1964. He obtained a B.S. degree from The Pennsylvania State University in 1986, a M.S. degree from Villanova University in 1988 and a Ph.D. degree from University of Pennsylvania in 1995, all in mechanical engineering. His doctoral research area was structural dynamics for continuous media with emphasis on wave propagation. Dominick has 30 years of precision electro-mechanical design experience specializing in piezoelectric transducers/actuators and robotic mechanisms. He is currently Fellow of Mechanical Engineering at Kulicke & Soffa Industries in Fort Washington, Pennsylvania, where he is globally responsible for the design of all ultrasonic transducers used for semiconductor wire bonding. Dominick holds six U.S. patents, and is also a licensed professional engineer.